

2006

Temporal Processing in the Exponential Integrate-and-Fire Model is Nonlinear

Joanna R. Wares

University of Richmond, jwares@richmond.edu

Todd W. Troyer

Follow this and additional works at: <http://scholarship.richmond.edu/mathcs-faculty-publications>



Part of the [Mathematics Commons](#), and the [Neurosciences Commons](#)

This is a pre-publication author manuscript of the final, published article.

Recommended Citation

Wares, Joanna R. and Troyer, Todd W., "Temporal Processing in the Exponential Integrate-and-Fire Model is Nonlinear" (2006). *Math and Computer Science Faculty Publications*. 51.

<http://scholarship.richmond.edu/mathcs-faculty-publications/51>

This Post-print Article is brought to you for free and open access by the Math and Computer Science at UR Scholarship Repository. It has been accepted for inclusion in Math and Computer Science Faculty Publications by an authorized administrator of UR Scholarship Repository. For more information, please contact scholarshiprepository@richmond.edu.

Temporal Processing in the Exponential Integrate-and-Fire Model is Nonlinear

Joanna Pressley and Todd W. Troyer

Applied Math and Scientific Computation Program

University of Maryland, College Park, MD 20742

Abstract

The exponential integrate-and-fire (EIF) model was introduced by Fourcaud-Trocme et al. (2003) as an extension of the standard leaky integrate-and-fire model (LIF). Here, the nonlinearity in the EIF model's temporal response to square-wave inputs is investigated. Comparing the time course of onset and offset responses revealed that offset responses have a steeper initial slope, but a slower approach to equilibrium. A linear systems analysis performed for these square-wave inputs indicates that at frequencies above ~40 Hz, gain was slightly smaller for square-wave inputs, but phase did not change significantly relative to simulations in which the corresponding sinusoids were presented in isolation.

Introduction

In their 2003 work, Fourcaud-Trocme et al formulated the exponential integrate-and-fire (EIF) neuron model, whose peri-threshold voltage dynamics more closely matched models containing an active sodium current [2]. They investigated the response of the EIF and other related models to sinusoidal inputs of varying amplitude and claimed that the model was well-approximated by a linear low-pass filter, for a range of inputs. The claim of linearity was based only on the fact that at each frequency, the gain of the response was independent of the amplitude injected.

To determine if the response of the EIF model continued to be linear for a broader range of inputs, we calculated the temporal response to square-wave currents constructed with a range of amplitudes and a range of baseline currents. In a linear model, the onset and offset responses should be identical except for the sign. Our basic finding is that onset responses show a slower

initial response but more rapidly reach the new equilibrium rate. We also compared the onset and offset response of the EIF model to the responses of the leaky integrate-and-fire (LIF) model. Generally, the EIF and LIF showed similar response patterns. The one substantial difference was that onset responses of the EIF model showed a greater delay relative to the LIF model. Finally, in a fully linear system, the response to a sum of inputs equals the sum of the responses to the individual inputs. To investigate this, we performed a Fourier analysis of the square-wave input and compared the resulting gain and phase calculated from the separate presentation of the component sinusoidal inputs. At higher frequencies, the gain for the square wave inputs was reduced relative to the sinusoids, while the phase of the response was remarkably similar across frequencies.

Methods

We constructed an EIF model as proposed by Fourcaud-Trocme et al [2]. The model consists of a passive leak conductance, g_L ($=0.1$ mS/cm²) plus an instantaneous voltage-dependent spiking current $\psi(V)$ that is activated near threshold:

$$C \frac{dV}{dt} = g_L (V_L - V) + \psi(V) + I(t) + \sigma \sqrt{C g_L} \eta(t)$$

$$\psi(V) = g_L \Delta_T \exp\left(\frac{V - V_T}{\Delta_T}\right)$$

V_L ($= -65$ mV) is the equilibrium potential of the leak, Δ_T ($=3.48$ mV) is the “spike slope factor” which determines the voltage sensitivity of the spiking current, and V_T ($= -59.9$ mV) is a voltage threshold at which the slope of the I-V curve vanishes and the equation becomes unstable. The membrane time constant ($= \tau = C / g_L$) was set at 10 msec. $\eta(t)$ is additive Gaussian noise (see below). Conceptually, spikes are triggered at the time at which voltage diverges to infinity. Practically, the time at which voltage crossed a triggering threshold ($= -30$ mV) was recorded, and the time from -30 mV to infinity was calculated analytically. After the spike, the voltage was

reset immediately to $V_{\text{AHP}} = -68$ mV, and voltage integration resumed after waiting for a refractory period of 1.7 msec.

The LIF model used identical parameters, except $\psi(V) = 0$. A spike was registered immediately when the voltage reached spike threshold, set at $V_T = -59.9$ mV. We found that by adding a 3.5 msec refractory period, the f-I curve matched that of the EIF model surprisingly well. The refractory period was implemented by resetting voltage to $V_{\text{AHP}} = -68$ mV, waiting 3.5 msec after the spike, and then resuming integration according to the equation:

$$C \frac{dV}{dt} = -g_L(V - V_L) + I(t) + \sigma \sqrt{Cg_L} \eta(t).$$

Simulations were performed in MATLAB (Mathworks, Natick, MA) using a using a 2nd order stochastic Runge-Kutta method [4] with step size ($dt = 2^{-4} = 0.0625$ msec). Noise currents $\eta(t)$ were assumed constant over each time step. The amplitudes of these currents were chosen from a zero-mean Gaussian distribution with standard deviation equal to 1. The noise power was determined by the parameter σ , which was set to 6.3 mV [2]. To more accurately simulate the rapid spike dynamics in the EIF model, during any time step in which voltage went above the voltage threshold, V_T , the dynamics were re-simulated using a reduced time step of $1/5 * 2^{-4} = 0.0125$ msec. (Noise currents were still assumed fixed over the larger 2^{-4} msec time step.)

Results

To assess the nonlinear components of response, we focused on input currents, $I(t)$, containing sharp onset and offset transients. In particular, the majority of our simulations used a 5 Hz square-wave input current. Initially, we compared the instantaneous firing rate of the model for the onset period and offset period, averaging 750,000 trials over bins of 1 msec. Figure 1A illustrates the histogram obtained from the EIF model for a baseline current of 0.25 nA and a 5

Hz square-wave input of 0.5 nA amplitude. If the response of the EIF was linear, the onset and offset response should have the same shape. However, the time course of these responses differs significantly (figure 1B). From these simulations, it appears that there are three stages of the response of EIF models to a transient step in input current. First, there is a period from one to several milliseconds in which the response to an onset transient is delayed. While rates do increase slightly during this period, the increase is slow. The response to the offset transient shows no such delay, and firing rate immediately shows a rapid decline. In the second stage, the response to both onsets and offsets changes rapidly, accounting for roughly 80% or more of the total change in rate. For the offset response, there is no noticeable distinction between these first two stages. In the third stage, the change in rate slows and eventually asymptotes at the steady state firing rate corresponding to the new level of current. It appears that the transition into this third, slowly changing stage happens earlier in time for the offset responses, and these rates approach asymptote more gradually. The response pattern for the LIF model is similar (figure 1C). However, the onset response does not show a distinct delay phase. Rather, both onset and offset responses change smoothly from baseline, but the onset response changes with a smaller slope.

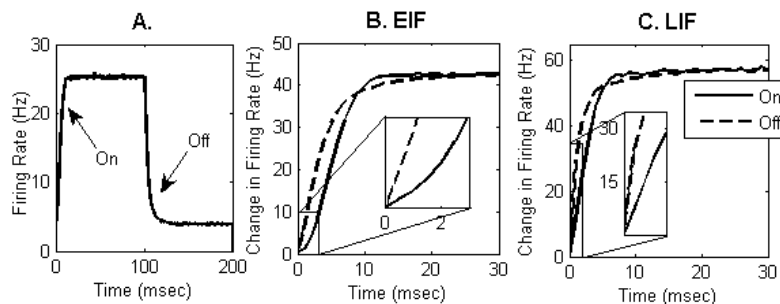


Figure 1: (A) The PSTH of the response of the EIF model to a square-wave input of 0.50nA with a baseline current of 0.25nA. (B) The onset and offset responses are depicted together for comparison. Inset shows the first 3 msec of the response. (C) The onset and offset responses for the LIF model to a square-wave input of 0.50 nA and a baseline current of 0.25nA. Inset shows the first 2 msec of the response

Parameter Dependence – Qualitative Results

To characterize the dependence of the onset/offset difference on the amplitude of the input changes, we held the baseline current constant and varied the amplitude of the square-wave currents. As expected, for all baseline currents the difference between the onset and offset responses grew as the amplitude of the square-wave was increased. The case where $I_0 = 0.25$ is delineated in figure 2A and 2C.

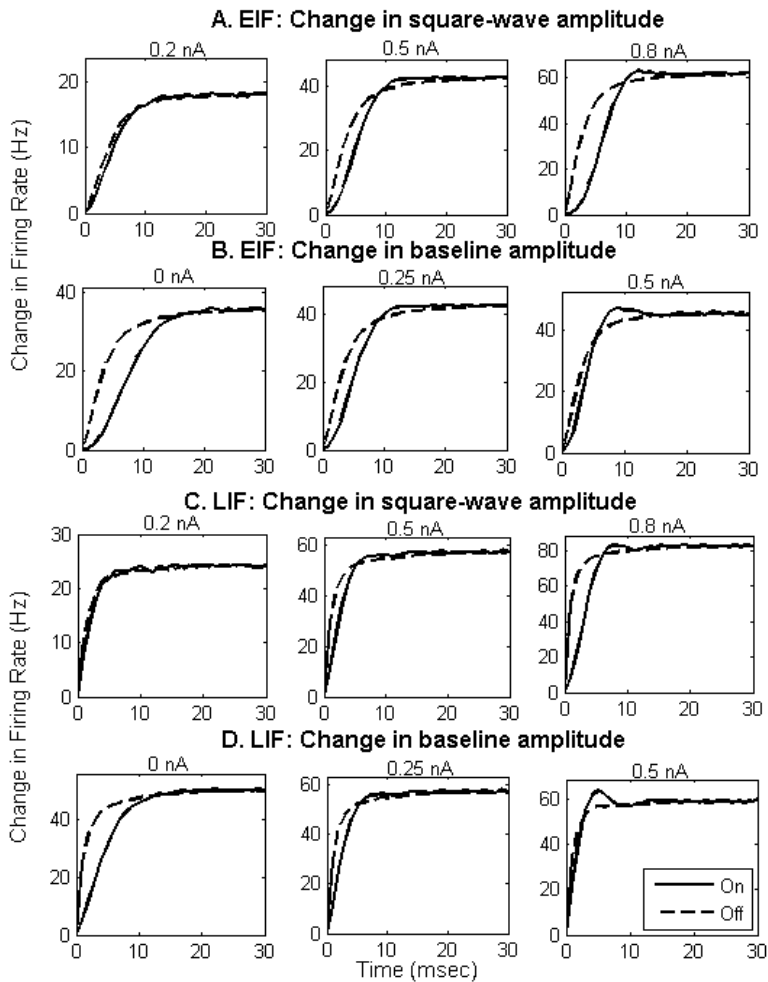


Figure 2: (A) The onset vs. offset responses for the baseline current $I_0 = 0.25$ nA. The amplitude of the square-wave is varied from 0.2 to 0.8 nA. The difference in the onset and offset responses grows as the amplitude of the square-wave grows. (B) The onset vs. offset responses for square-wave current with amplitude 0.5 nA and baseline currents varying from 0.25 to 1 nA. (C) Same as A except for the LIF instead of the EIF model. (D) Same as B except for the LIF instead of the EIF model.

Next, we varied the baseline current while holding the amplitude of the square-wave current constant. Figure 2B and 2D depict the case where the baseline is 0.5 nA and the amplitude of the square-wave is varied from 0 to 0.50 nA. The slopes of the initial response for the onset and offset differ less as the baseline current is increased. However, as the baseline current is increased, the neuron moves between the “random firing” regime, in which the mean current is sub-threshold and spikes are driven by random threshold crossings, and the “regular firing” regime in which the mean current is above threshold and the model produces regular trains of action potentials as the voltage is integrated up to threshold [1, 6]. As the neuron moves into the regular firing regime, its response to a step change causes a predilection for spiking synchronously, creating an oscillation in the firing rate (figure 2B,D last box) [3]. It is unclear whether an over-damped version of this oscillation is related to the faster approach to the new firing rate demonstrated in the onset responses across the range of input parameters.

Parameter Dependence – Quantitative Results

To more systematically examine how the response changes to changes in the amplitude and baseline of the input, we fit the onset and offset curves with the two-parameter hyperbolic ratio: $f(t) = \frac{t^n}{t^n + c^n}$. To enable the fit, we normalized the curves by dividing by the difference in equilibrium firing rates. The c parameter is most associated with the delay: time t equals c marks the time at which responses are midway between the new and old rates. The n parameter is associated with the steepness of the response, with a larger value of n meaning a steeper response function. When the regime starts switching to the regular firing regime, the response exhibits synchrony effects and this function no longer fits well. However, even though the function cannot fit the oscillations seen in this regime, it still fits the initial phases of the response, as well as doing a reasonable job of characterizing the overall approach to the new firing rate.

Figure 3 shows the values of the best-fit parameters as a function of square-wave amplitude for both low (dashed) and higher (solid) levels of the baseline current. The plots on the left show that increasing the amplitude affects the delay parameter c in opposite directions, increasing the delay for onset responses and reducing the delay for offset responses. Similar patterns are seen for high and low baseline simulations in both the EIF and LIF models, although high baseline currents and the LIF model are associated with lower delay overall. Increasing amplitude also causes an increasing difference in the steepness parameter n for both the EIF and LIF models at high and low gain (right). However, unlike the delay parameter, changes in the steepness parameter are much more pronounced for the onset response; the offset response shows little change in n across parameters.

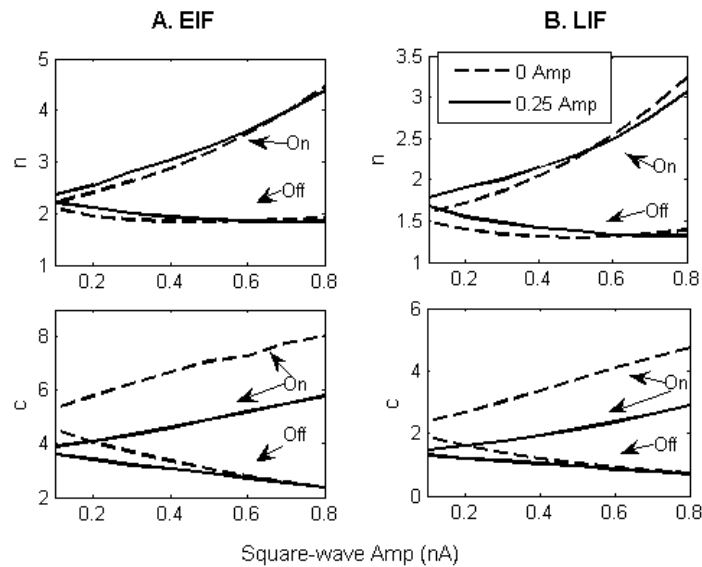


Figure 3: (A) The EIF model's onset and offset responses are fit with the equation $f(t) = \frac{t^n}{t^n + c^n}$ and the parameters of $f(t)$ are plotted for square-wave currents with amplitudes varying (x-axis) from 0.2 to 0.8. The parameters are plotted for 0nA (dotted line) and 0.25nA (solid line) baseline currents. (B) Same as A for the LIF model.

Fourier Analysis

Finally, we disassembled the square-wave input and resulting output into their Fourier components and calculated the gain and phase for each component. We then presented the sinusoidal components individually and calculated the gain and phase. The comparison between the two calculations for a baseline current of 0 nA is shown in figure 4. For the model to act linearly, the response of the sums of inputs should be equal to the sum of the responses of the inputs. For low frequencies, the gain and phase for square-wave and sinusoidal inputs are very similar. But as the frequencies increase above approximately 40 Hz, the gains of the responses diverge. Near 100 Hz, the gain using the EIF model for square-wave inputs is nearly 25% lower than for the corresponding sinusoids and for the LIF model the gain is around 10% lower for the square-wave components. (The low gain found at higher frequencies resulted in less reliable measurements of gain and so these results are not shown.)

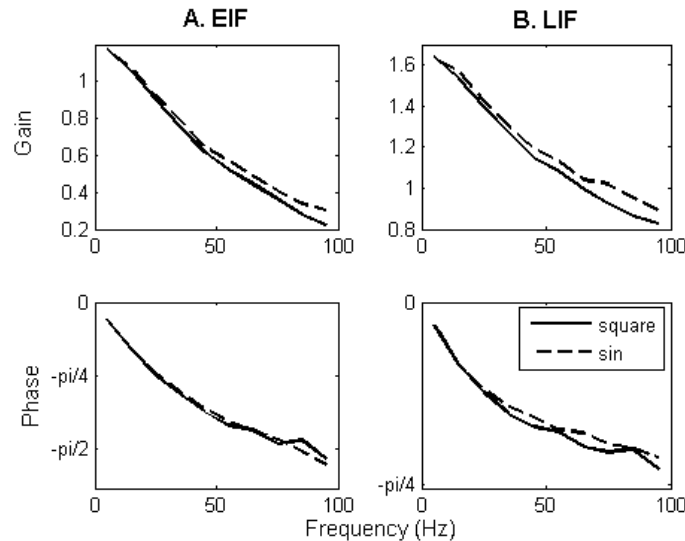


Figure 4: (A) The gain and phase of the EIF's response to the square-wave Fourier components and corresponding sinusoidal inputs for a baseline of 0 nA and a square-wave of 0.3 nA. (B) Same as A for the LIF model.

Discussion

Our results indicate that the temporal response of both the EIF and LIF models have a significant nonlinear component. In particular, offset transients have a more rapid onset followed by a slower decay as compared to onset transients. The difference between the onset and offset responses increases as the amplitude of the square-wave input is increased. Additionally, the gain due to the Fourier components of the square-wave response do not match the corresponding gain of the response to the sinusoids presented individually, especially for higher frequencies. With our parameters, the difference becomes pronounced above about 40 Hz. Although linear analyses can be a useful first step in characterizing the dynamic responses of model neurons, these results argue for a cautious interpretation of the results. More complete characterizations will require a parametric exploration of the dynamic range over which the analysis is valid and/or an exploration of a wider range of stimuli than simple sinusoids.

Our study using square-wave inputs revealed three basic nonlinearities in the response of integrate-and-fire models. The most striking non-linearity is a delay in the onset response of the EIF model. This delay is not seen during offset responses or in either onset or offset responses of the LIF model. We speculate that this delay relates to time it takes for trajectories to travel from the voltage to infinity to be registered as a spike. The second basic nonlinearity is the slightly reduced slope in the rapidly changing phase of the response for onsets relative to offsets. In the LIF model, this is the main effect that makes the initial stage of onset responses slower than offset responses. Finally, a third nonlinearity is seen that results in offset responses returning more slowly to the new steady state firing rates than onset responses. Currently, it is unclear whether these different stages of the response should be considered distinct dynamical mechanisms, or whether they result from a single dynamical process unfolding over time.

References

- [1] M. Abeles, *Corticonics: Neural Circuits of the Cerebral Cortex* (Cambridge University Press, New York, 1991).
- [2] N. Fourcaud-Trocmé, D. Hansel, C. van Vreeswijk, and N. Brunel, How Spike Generation Mechanisms Determine the Neuronal Response to Fluctuating Inputs, *The Journal of Neuroscience* 23 (2003) 11628-11640.
- [3] W. Gerstner, Population Dynamics of Spiking Neurons: Fast Transients, Asynchronous States, and Locking, *Neural Computation* 12 (2000) 43-89.
- [4] R. L. Honeycutt, Stochastic Runge-Kutta algorithms I. White noise, *Physical Review A* 45 (1992) 600-603.
- [5] T. W. Troyer, Rate Dynamics in Integrate-and-Fire Neurons: Two Regimes and Multiple Time Scales, *CNS2001*, Monterrey, 2001.
- [6] T. W. Troyer and K. D. Miller, Physiological Gain Leads to High ISI Variability in a Simple Model of a Cortical Regular Spiking Cell, *Neural Computation* 9 (1997) 971-983.